

# Numerical computation of relative equilibria with Femlab

V. Thümmler

Fakultät für Mathematik, Universität Bielefeld.

e-mail: [thuemmler@math.uni-bielefeld.de](mailto:thuemmler@math.uni-bielefeld.de)

## Abstract

Relative equilibria are special solutions of partial differential equations (PDEs), which are stationary in an appropriate comoving frame of reference. Such solutions occur frequently in biological and chemical models, e.g. when describing pattern formation of reaction-diffusion equations. Examples are traveling waves in 1d, planar and spiral waves in 2d and scroll waves in 3d. If the equation has a special symmetry property - equivariance, then one can transform the equation into the comoving frame during the computation of the solution. We will show that this can be very convenient for numerical computations. We have implemented the resulting “frozen equation” in Femlab and conducted several numerical experiments for different examples in 1d and 2d such as traveling waves and spirals in the FitzHugh-Nagumo and the complex Ginzburg-Landau system. Moreover, we describe some of the problems which arise because of the additional convective terms which have been introduced by the freezing transformation.

## 1 Introduction

The simplest examples of relative equilibria are traveling wave solutions of parabolic PDEs (e.g. reaction-diffusion equations)

$$u_t = Du_{xx} + f(u), \quad u(\cdot, 0) = u^0, \quad x \in \mathbb{R}, \quad u(x, t) \in \mathbb{R}^m, \quad D \in \mathbb{R}^{m,m}.$$

These are solutions of the form  $u(x, t) = \bar{v}(x - \bar{\lambda}t)$ , where the waveform  $\bar{v}$  does not depend on time and  $\bar{\lambda} \in \mathbb{R}$  is the velocity of the wave. Via the ansatz  $u(x, t) = v(x - \gamma(t), t)$ ,  $\lambda(t) = \gamma'(t)$  and by adding a phase condition which compensates for the additional degree of freedom, the PDE can be transformed into a partial differential algebraic equation (PDAE) of the form

$$\begin{aligned} v_t &= Dv_{xx} + f(v) + \lambda v_x, \quad v(\cdot, 0) = u^0, \quad \lambda(0) = \lambda^0 \\ 0 &= \psi(v, \lambda). \end{aligned} \tag{1}$$

Note, that there are different possible choices for the phase condition  $\psi$ , which we will discuss later. In this framework the traveling wave  $(\bar{v}, \bar{\lambda})$  is a stationary solution and the method is a transient method, i.e. during time evolution, the solution of (1) converges to  $(\bar{v}, \bar{\lambda})$ .

Using this method of “freezing” makes it possible to observe phenomena which are visible after a transient phase only, whereas by direct numerical simulation e.g. a traveling wave leaves the finite domain of computation after short time.

## 2 Methods

The general approach [2],[8] is not restricted to traveling waves, but includes for example rotating waves in 1d or spiral waves in 2d. We will describe this approach using the more abstract setting of an evolutionary equation in a Banachspace  $X$  (e.g.  $X = L_2$ ,  $X = BC_{unif}$ )

$$u_t = F(u), \quad u(0) = u^0, \quad (2)$$

which satisfies the equivariance relation  $F(a(\gamma)u) = a(\gamma)F(u)$ , where  $a$  denotes the action of a finite dimensional Lie group  $G$  on  $X$

$$\begin{aligned} a : G &\rightarrow GL(X), \quad \gamma \mapsto a(\gamma), \text{ where} \\ a(\gamma_1 \circ \gamma_2) &= a(\gamma_1)a(\gamma_2), \quad a(e) = I, \quad e = \text{unit element in } G. \end{aligned}$$

Examples are

$$G = \mathbb{R}, \quad [a(\gamma)u](x) = u(x - \gamma) \quad (3)$$

$$G = \mathbb{R} \times S^1, \quad \gamma = (\tau, \omega), \quad [a(\gamma)u](x) = \exp(-i\omega)x(x - \tau) \quad (4)$$

$$\begin{aligned} G &= SE(2) = S^1 \ltimes \mathbb{R}^2, \quad \gamma = (\rho, \tau), \quad \gamma_1 \circ \gamma_2 = (\rho_1 + \rho_2, \tau_1 + R_{\rho_1}\tau_2), \\ [a(\gamma)u](x) &= u(R_{-\rho}(x - \tau)) \end{aligned} \quad (5)$$

where  $R_\rho = \begin{pmatrix} \cos(\rho) & -\sin(\rho) \\ \sin(\rho) & \cos(\rho) \end{pmatrix}$  is a rotation matrix.

Again, we use a separation ansatz  $u(t) = a(\gamma(t))v(t)$ , which decouples the motion of the solution form (e.g. the wave form) from the motion which is due to the group operation (e.g. translation). In order to single out a unique solution from the whole family of solutions an additional constraint - a so called phase condition - is added and equation (2) is transformed into

$$\begin{aligned} v_t &= F(v) - [da(e)v]\lambda \\ \gamma_t &= dL_\gamma(e)\lambda \\ 0 &= \psi(v), \end{aligned} \quad (6)$$

where  $da(e)$  denotes the derivative of the action  $a$  w.r.t.  $\gamma$  at the unit element  $e \in G$  and  $dL_\gamma$  denotes the derivative of the left multiplication with  $\gamma$  (for more details see [10]). The equation for the group element  $\gamma$  describes the motion along the group and is decoupled from the other equations.

To be more specific, for a parabolic equation  $u_t = D\Delta u + f(u, \nabla u)$  we obtain from the first and the second equation of (6) the form:

$$\begin{aligned} v_t &= D\Delta v + f(v, \nabla v) - S(v, \nabla v)\lambda, & x \in \Omega, t \geq 0 \\ 0 &= \psi(v, \nabla v) \end{aligned} \quad (7)$$

where  $S(v, \nabla v)\lambda = \sum_{i=1}^d S_i(v, \nabla v)\lambda_i$ ,  $d = \dim(G)$  and where we denoted the realization of the phase condition again with  $\psi$ . We assume that the  $S^i$  are linear differential operators of order  $\leq 1$  which can be written as

$$S_i(v, \nabla v)(x) = S_i^0(x)v(x) + S_i^1(x)\nabla v(x), \quad S_i^{0,1}(x) \in \mathbb{R}^{m,m}.$$

The phase condition leaves some freedom of choice. We consider the following two possibilities

$$\psi_{\text{fix}}(v) = \int_{\Omega} S(v^0, \nabla v^0)^T (v - v^0) dx \quad \text{and} \quad \psi_{\text{orth}}(v, \nabla v) = \int_{\Omega} v_t^T S(v, \nabla v) dx.$$

The first condition fixes the solution w.r.t. the initial value  $v^0$ . This requires that the initial value has to be chosen in such a way that the regularity of the phase condition is guaranteed. Alternatively one can use a given template function instead of  $v^0$ . The second condition enforces the minimization of the temporal change of the shape  $\|v_t\|_{L_2}$ .

### 3 Implementation

The PDAE (7) is implemented in Femlab by coupling a general PDE mode to a to a boundary mode (in 1d) or a weak point mode (in 2d) which enforces the phase condition. For  $\psi_{\text{fix}}$  another mode is added for the template function. The coupling between the constraint and the other equations is implemented by using coupling integration variables. In all computations we used quadratic lagrange elements (linear elements give similar results).

### 4 Numerical Results

We illustrate the method on different examples in 1d and 2d FitzHugh-Nagumo and the complex Ginzburg-Landau system. These systems describe different aspects of signal propagation in heart tissue and exhibit different patterns such as traveling waves, spirals and rotating vortices. [4], [3].

## 4.1 QCGL, 1d

The cubic quintic Ginzburg Landau equation [9],[11]

$$u_t = \alpha u_{xx} + \delta u + f(u), \quad f(u) = \beta|u|^2u + \gamma|u|^4u, \quad \delta \in \mathbb{R}, \alpha, \beta, \gamma \in \mathbb{C} \quad (8)$$

in one space dimension shows a variety of coherent structures, like stable pulse solutions, fronts, sources, sinks, etc. . Moreover, the equation has regimes where the behavior is intrinsically chaotic. For certain parameter values this equation exhibits stable rotating pulses [9] and unstable pulses, as well as rotating and traveling fronts. All these solutions can be written in the form

$$u(x, t) = \exp(-i\bar{\lambda}_\rho t)\bar{v}(x - \bar{\lambda}_\tau t).$$

The equation (8) is equivariant w.r.t. the group  $G = S^1 \times \mathbb{R}$  given in (4). Therefore using the Ansatz  $u(x, t) = \exp(-i\gamma_\rho(t))v(x - \gamma_\tau(t))$ ,  $\gamma'_\tau = \lambda_\tau$ ,  $\gamma'_\rho = \lambda_\rho$  and adding e.g. the fixing phase condition  $\psi_{\text{fix}}$  we obtain

$$\begin{aligned} v_t &= \alpha v_{xx} + \delta v + f(v) + \lambda_\tau v_x + i\lambda_\rho v, \\ 0 &= \langle v_x^0, v - v^0 \rangle_{L_2}, \quad 0 = \langle iv^0, v - v^0 \rangle_{L_2} \end{aligned} \quad (9)$$

i.e. the additional symmetry terms are given by  $S(v)\lambda = \lambda_\tau v_x + i\lambda_\rho v$ ,  $\lambda = (\lambda_\tau, \lambda_\rho)$ . For the parameter set  $a = 1, d = -0.1, b = 3 + i, g = -2.75 + i$  [9], one can see on the left of Figure 1 a stable rotating pulse evolve due to equation (8) (the real part is shown). On the right you see the computation for equation (9). After a short transient time, the wave form stabilizes and the rotational velocity  $\lambda_\rho$  and the translational velocity  $\lambda_\tau$  become constant, as shown in Figure 2.

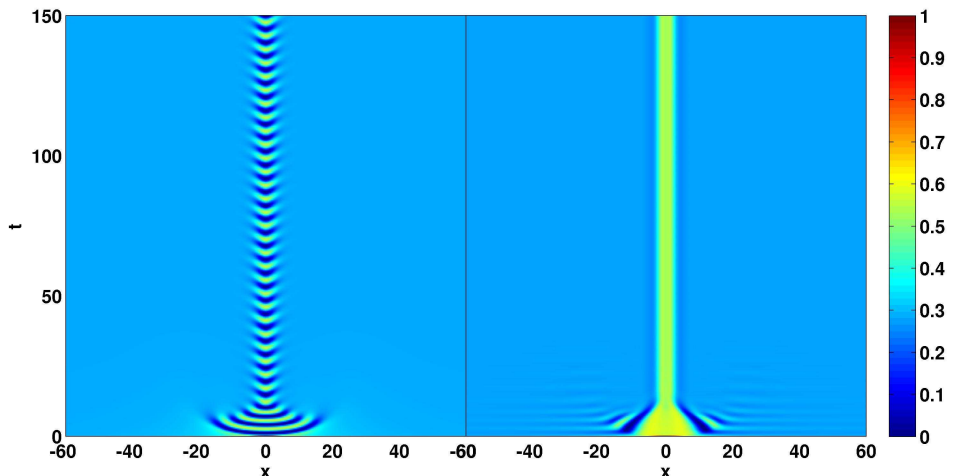


Figure 1: QCGL, rotating vs. frozen wave, real part

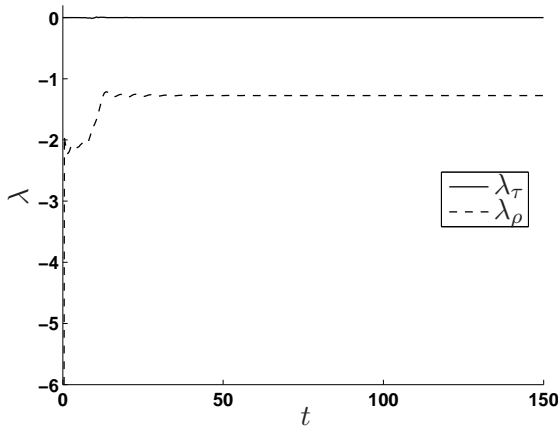


Figure 2: QCGL, time evolution of  $\lambda$

## 4.2 FHN 1d

The well known FitzHugh-Nagumo system

$$\begin{aligned} u_t &= \Delta u + u - \frac{1}{3}u^3 - v, \\ v_t &= \phi(u + a - bv) \end{aligned}$$

which models nerve conduction, is equivariant w.r.t. translation and possesses traveling wave solutions [6], [7]. Thus the transformed equation is given by (7). We used the parameters  $a = 0.7$ ,  $b = 0.8$ ,  $\phi = 0.08$  and Neumann boundary conditions on an interval  $[0, 130]$  with  $hmax = 0.5$ .

In Figure 3 the time evolution of the  $u$ -component of a given initial profile ( $v$  has been set initially to the stationary value -0.62426) is shown. The initial hump splits into two traveling components and after some time only the left moving pulse exists which finally leaves the computational window. In Figure 4 the results of the “freezing method” with the two different phase conditions are compared. If the orthogonality phase condition  $\psi_{\text{orth}}$  is used, then the left moving pulse is frozen, whereas the right moving pulse stabilizes at the position of the initial hump if the fixing phase condition  $\psi_{\text{fix}}$  is used. Correspondingly  $\lambda$  converges to velocities of opposite sign.

As we see in this example, our method can only freeze one wave at a time. Which one is selected, depends on the type of phase condition used.

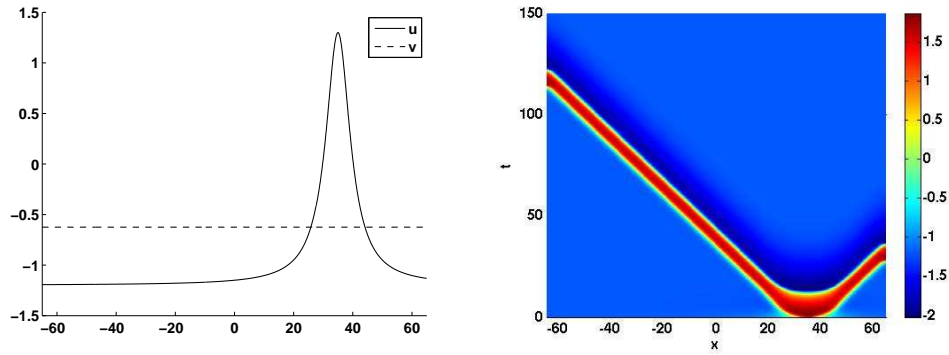


Figure 3: FHN, initial values, traveling wave

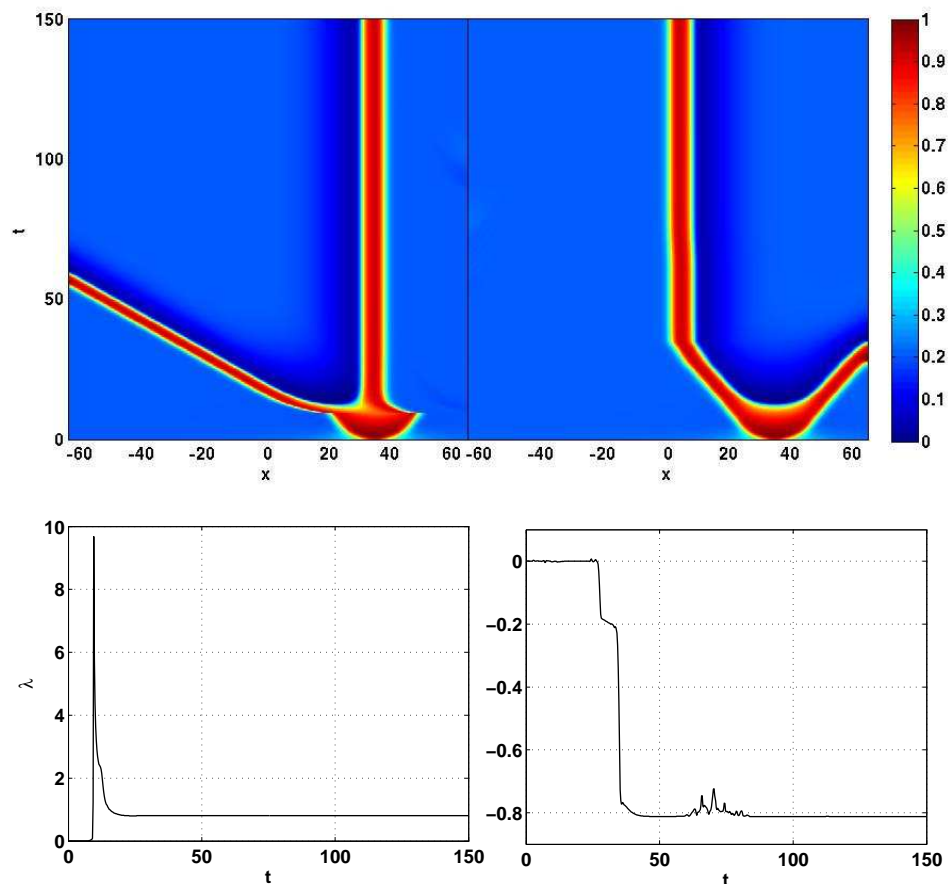


Figure 4: FHN, different phase conditions, time evolution of  $u$  and  $\lambda$

### 4.3 QCGL 2d

The 2d quintic Ginzburg Landau system (8) possesses strongly localized solutions, so called spinning solitons. These occur at parameter values  $a = (1 + i)/2$ ,  $d = 1/2$ ,  $b = 2.5 + i$ ,  $g = -1 - 0.1i$ , see [5]. This equation is equivariant w.r.t. to the action  $\alpha$  of the four dimensional group  $SE(2) \times S^1 \ni \gamma = (\rho, \tau, \omega)$ ,  $\tau = (\tau_x, \tau_y)$ , given by

$$[a(\gamma)v] \left( \begin{array}{c} x \\ y \end{array} \right) = \exp(i\omega)v(R_{-\rho} \left( \begin{array}{c} x \\ y \end{array} \right) - \left( \begin{array}{c} \tau_x \\ \tau_y \end{array} \right)))$$

leading to the symmetry terms  $S(v)\lambda = \lambda_1(xv_y - yv_x) + \lambda_2v_x + \lambda_3v_y + \lambda_4iv$ .

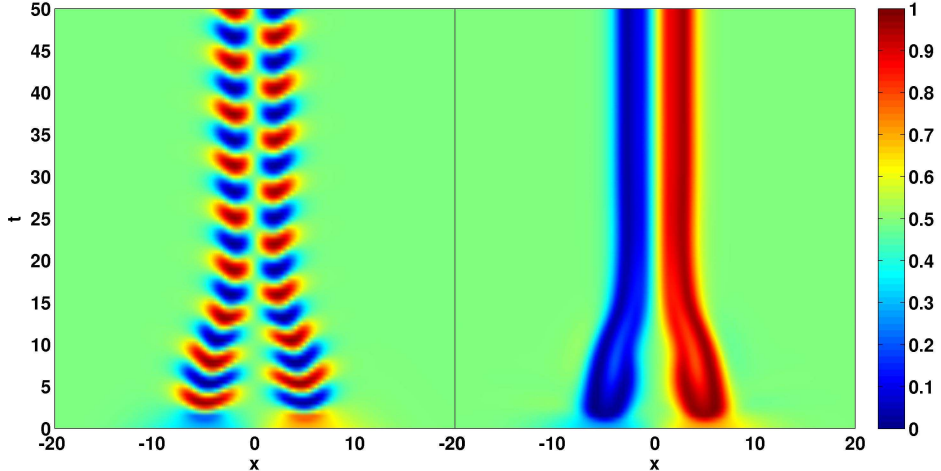


Figure 5: QCGL, rotating vs. frozen wave

With the numerical parameters  $R = 20$ ,  $hmax = 1$ , we start at an initial profile that is given in polar coordinates  $(r, \varphi)$  by  $u_0(r, \varphi) = 0.2 \exp(i\varphi)r \exp(-(r/7)^2)$ . Then solving (8) directly, a localized vortex solution develops the real part of which is displayed in the left of Figure 6. On the left of Figure 5 the corresponding time evolution of a slice along the x-axis is shown. On the right you see the same for the computation of the frozen system.

After a short transient time the algebraic variables stabilize at fixed values, the translational velocities becoming zero.

A similar computation has been carried out for a slightly different value of  $b = 2.6 + i$ . Here a rotating spiral develops, the time evolution of which is shown in Figure 8. Since here we started from the spiral profile, the algebraic variables converge to the stationary values very fast, where again the translational velocities are zero.

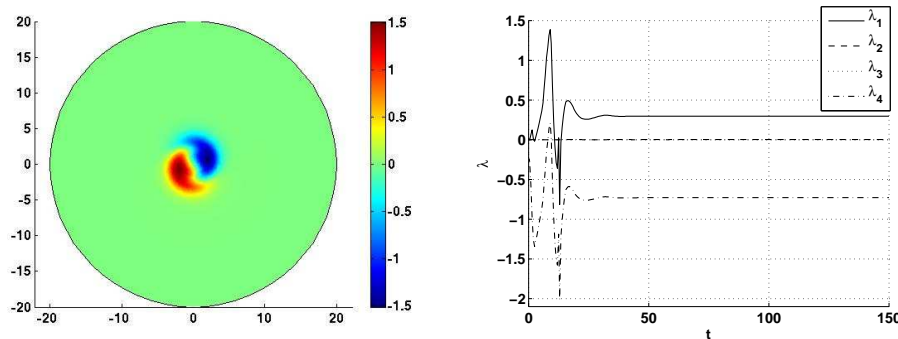


Figure 6: QCGL, real part of rotating wave at  $t=150$ , time evolution of  $\lambda$

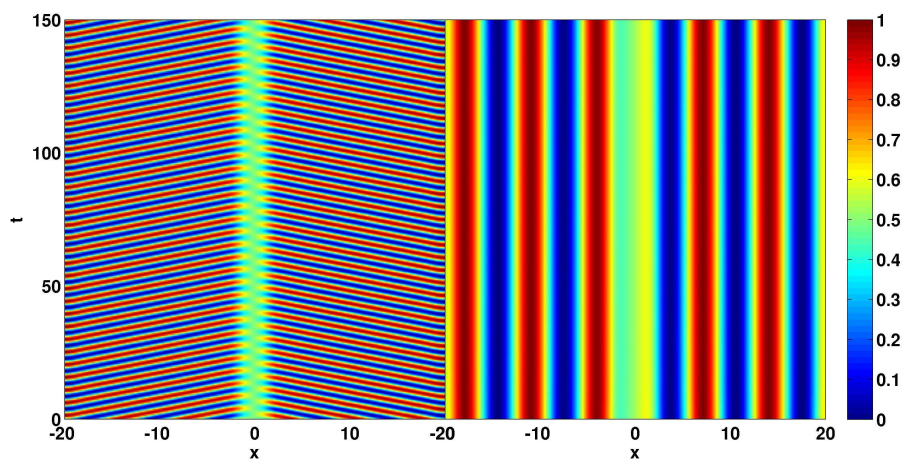


Figure 7: QCGL, rotating vs, frozen wave

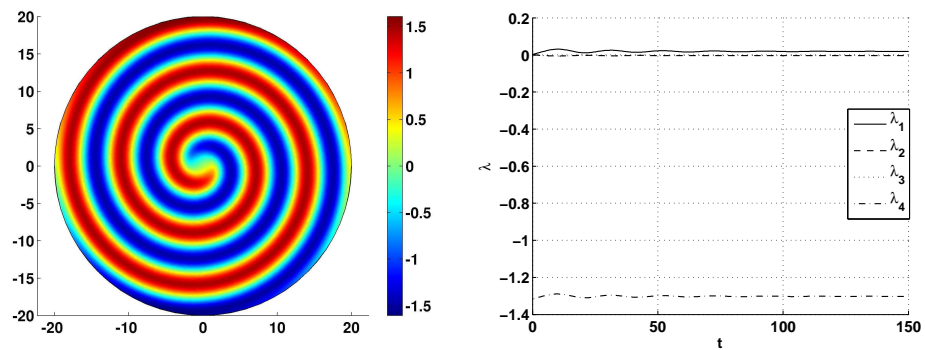


Figure 8: QCGL, real part of initial value, time evolution of  $\lambda$

#### 4.4 Barkley 2d

The last example is the well known Barkley system which is a variant of the FHN system [1] given by

$$u_t = \Delta u + \frac{1}{\epsilon} u(1-u)(u - \frac{v+b}{a}) \\ v_t = d\Delta v + u - v.$$

The equation is equivariant with respect to the action of  $SE(2)$ , (see (5)), and we have  $S(v)\lambda = \lambda_1(xv_y - yv_x) + \lambda_2v_x + \lambda_3v_y$ .

We test our method in the parameter regime of rigidly rotating spirals with  $\epsilon = \frac{1}{50}$  and  $a = 0.75$ ,  $b = 0.01$ ,  $d = 0.1$ .

Since the diffusion term in the second equation is relatively small, leading to a system of mixed hyperbolic-parabolic type for  $d = 0$ , the use of a stabilization method is essential. Thus we coupled two convection-diffusion modes for  $u$  and  $v$  with a weak point mode which enforces the phase condition. As shown in Figure 9, after some initial oscillations the solution stabilizes for the frozen system. The time evolution of the corresponding algebraic variables is shown in Figure 10. We

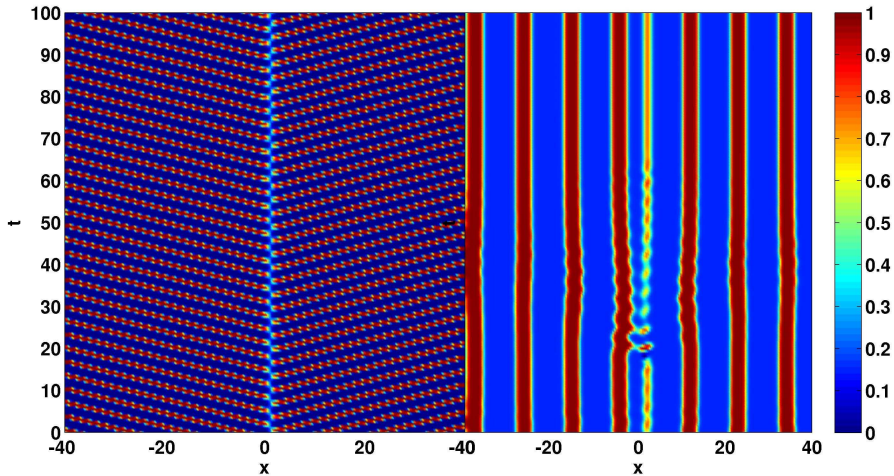


Figure 9: Barkley, rotating vs. frozen wave

observed difficulties when decreasing  $d$  further to zero. Then the large convective terms at the boundary become effective and destroy the solution after a short time.

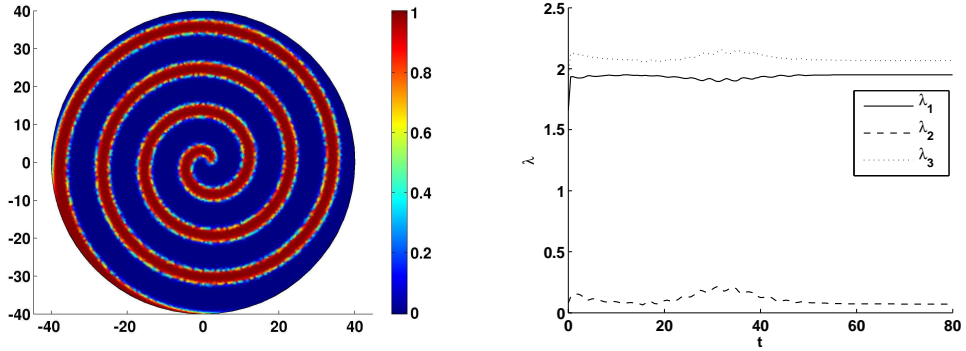


Figure 10: Barkley,  $u$ -component of initial value, time evolution of  $\lambda$

## 5 Conclusions

We have presented a method which enables to compute relative equilibria as stationary solutions of a transformed system via a transient method. Using the time dependent solver for the ‘‘freezing’’ one can obtain initial values for the stationary solver. These stationary solutions can then be continued w.r.t. to a system parameter by using the parametric solver.

## References

- [1] D. Barkley. Euclidean symmetry and the dynamics of rotating spiral waves. *Phys. Rev. Lett.*, 72:164–167, 1994. 9
- [2] W.-J. Beyn and V. Thümmler. Freezing solutions of equivariant evolution equations. *SIAM Journal on Applied Dynamical Systems*, 3(2):85–116, 2004. 2
- [3] V. N. Biktashev. Dissipation of the excitation wave fronts. *Phys. Rev. Lett.*, 89(16):168102, Sep 2002. 3
- [4] D. Bini, C. Cherubini, and S. Filippi. Viscoelastic Fitzhugh-Nagumo models. *Physical Review E*, 72, 2005. 3
- [5] L.-C. Crasovan, B. A. Malomed, and D. Mihalache. Spinning solitons in cubic-quintic nonlinear media. *Pramana Journal of Physics*, 57(5/6):1041–1059, 2001. 7

- [6] R. M. Miura. Accurate computation of the stable solitary waves for the FitzHugh-Nagumo equations. *Journal of Mathematical Biology*, 13:247–269, 1982. 5
- [7] J. D. Murray. *Mathematical biology*, volume 19 of *Biomathematics*. Springer-Verlag, Berlin, second edition, 1993. 5
- [8] C. W. Rowley, I. G. Kevrekidis, J. E. Marsden, and K. Lust. Reduction and reconstruction for self-similar dynamical systems. *Nonlinearity*, 16(4):1257–1275, 2003. 2
- [9] O. Thual and S. Fauve. Localized structures generated by subcritical instabilities. *J. Phys. France*, 49:1829–1833, 1988. 4
- [10] V. Thümmler. Numerical approximation of relative equilibria for equivariant PDEs. Preprint no. 05-017 of the CRC 701, Bielefeld University, 2005. 3
- [11] W. van Saarloos and P. C. Hohenberg. Fronts, pulses, sources and sinks in generalized complex Ginzburg-Landau equations. *Phys. D*, 56(4):303–367, 1992. 4